Molecular dynamics simulations of enhanced Green Fluorescent Proteins: Effects of F64L, S65T and T203Y mutations on the ground-state proton equilibria

ARTICLE *in* PROTEINS STRUCTURE FUNCTION AND BIOINFORMATICS · MAY 2003

Impact Factor: 2.63 · DOI: 10.1002/prot.10335 · Source: PubMed

2 AUTHORS:

Riccardo Nifosì
Italian National Research Council
50 PUBLICATIONS **951** CITATIONS
SEE PROFILE

Valentina Tozzini
Italian National Research Council
74 PUBLICATIONS **1,993** CITATIONS
SEE PROFILE

Molecular Dynamics Simulations of Enhanced Green Fluorescent Proteins: Effects of F64L, S65T and T203Y Mutations on the Ground-State Proton Equilibria

R. Nifosì and V. Tozzini
NEST-INFM and Scuola Normale Superiore, Piazza dei Cavalieri 7, I-56126 Pisa, Italy

ABSTRACT **Molecular dynamics simulations with the Amber force field are carried out to study two mutants of the green fluorescent protein (GFP), namely EGFP (F64L/S65T) and T203Y-EGFP (E^2GFP). Those variants display an opposite equilibrium between the structural A and B states, associated with neutral and anionic protonation forms of the chromophore. Configurations of those two states are simulated for each variant and the energetics of their equilibrium in the two mutants is studied by evaluating the change in the relative free energy of A and B states (ΔG_{AB}) upon T203Y mutation. The resulting $\Delta\Delta G_{AB}$ agrees with the value inferred from absorption measurements. A comparison of the hydrogen bond network around the chromophore rationalizes the different population of state A and B in EGFP and E^2GFP. On the basis of structural and energetic considerations, a mechanism for destabilization of the neutral chromophore in S65T mutants is proposed. Simulations of the B state of the S65T variant and of WT GFP are also performed for comparison and to test the force field parameters of the chromophore derived for the present calculations. Possible paths of proton transfer leading to nonfluorescent states of the chromophore are discussed in light of the photodynamical behavior of GFP, as revealed by fluorescence correlation spectroscopy and single-molecule experiments. Proteins 2003;51:378–389.** © 2003 Wiley-Liss, Inc.

Key words: GFP; molecular dynamics simulations; proton equilibria; photodynamics

INTRODUCTION

In the last decades, the green fluorescent protein (GFP) of the jellyfish *Aequorea victoria* has found countless applications in cell biology, biochemistry, and biotechnology. The ability to fluoresce without the need of any external co-factor and the absence of interference with the function of the tagged protein[1] make GFP an ideal marker of gene expression and protein trafficking in living cells. Moreover, GFP shows high thermal stability and good quantum yield thanks to its rigid β-barrel fold protecting the chromophore,[2,3] generated by an autocatalytic cyclization and subsequent oxidation of three adjacent residues (Ser65, Tyr66 and Gly67).[1] This mechanism, whose efficiency is a key ingredient in GFP functionality, produces a *p*-hydroxybenzylindene-imidazolidinone, constituted by the phenolic ring of Y66 linked to an imidazolidinone ring by a bridging carbon (see Fig. 1).

The absorption spectrum of wild type (WT) GFP consists of a major band at 395 nm (A) and a minor one at 475 nm (B). On the basis of structural analyses[1,4,5] these bands are attributed to different forms of the chromophore, differing in the protonation of the hydroxyl group of the phenolic ring, protonated in the more populated state (corresponding to peak A) and deprotonated in the minor one (peak B). To date no experimental evidence for protonation of the imidazolidinone nitrogen has been found,[6] and the bright A and B states are generally assigned to the neutral and anionic chromophore, respectively. States having the imidazolidinone nitrogen protonated (namely the cation and the zwitterion) were proposed as possible nonemitting dark states.[7,8] The fluorescence of WT GFP peaks at 505 nm and is almost entirely due to the emission of the anionic chromophore. Indeed, when the A state (with a neutral chromophore) is excited, the phenolic moiety loses the proton, leading to the fluorescence of the anionic species. The destination of the involved proton is somewhat debated, the current hypothesis being that it is transferred to the carboxylate group of Glu222 through a network of H-bonds in the chromophore environment.[4] The state resulting from the proton transfer, usually called I, is supposed to be intermediate between the A and B states, namely having the anionic chromophore in an unrelaxed environment, more similar to that of state A.[4]

Several GFP mutants have been developed with improved photostability and different spectral properties, such as blue or red shifted emission. The double F64L/S65T mutant, called Enhanced GFP (EGFP), is the most widely used in molecular and cell biology. F64L mutation improves folding efficiency, whereas S65T yields an excitation spectrum with a maximum peak at 490 nm, which is more suitable for use in living cells being less energetic than the 395 nm excitation needed for WT GFP.[9] The side chain of residue at position 65, though not directly involved in the double ring structure of the chromophore, is located in close contact with the imidazolidinone ring and with Glu222. Because Glu222 is supposed to be anionic in

*Correspondence to: Riccardo Nifosì, NEST-INFM and Scuola Normale Superiore, Piazza dei Cavalieri 7, I-56126 Pisa, Italy. E-mail: r.nifosi@nest.sns.it.

Received 26 July 2002; Accepted 25 October 2002

Published online 00 Month 2002 in Wiley InterScience (www.interscience.wiley.com). DOI: 10.1002/prot.10335

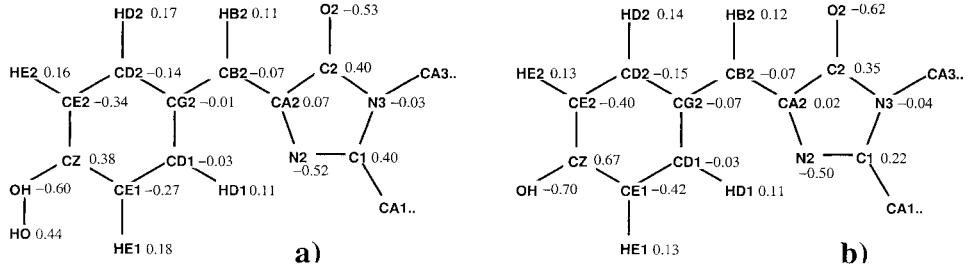

Fig. 1. (a) neutral form of the chromophore. For each atom the calculated partial charge is reported together with the PDB name. Panel (b) is the same as (a) for the anionic form.

the A state, the presence of close H-bond donors is crucial in stabilizing its negative charge. Perturbation of the H-bond network around Glu222 may lead to destabilization of the A state in favor of the B state, as is the case for S65T and EGFP. Mutants exhibiting yellow fluorescence (so called YFP) were obtained by inserting residues at position 203 (T203Y/F), which interact by aromatic stacking with the phenolic ring of the chromophore.[10] Moreover, mutation of threonine at position 203 into tyrosine or phenylalanine subtracts a H-bond donor to the phenolate of the chromophore. The aromatic stacking interaction together with a less well-coordinated anionic chromophore are responsible for the red-shifted fluorescence and absorption of the B state of these mutants.[11] When the mutations described above are combined together, like in the so-called E^2GFP variant (F64L/S65T/T203Y), an equilibrium population is restored that is similar to that of the wild type, i.e., with a larger population of the A state.[12]

Only some of the several known GFP variants—including WT GFP,[3] S65T,[2,4] and yellow mutants (S65G/V68L/S72A/T203Y and S65G/V68L/S72A/T203Y/H148G)[10]—were studied by X-ray spectroscopy, providing the basis for the explanation of many aspects of their optical properties. These structures constitute a set wide enough to model other mutants with high sequence homology. In this article, we present a molecular dynamics (MD) analysis starting from atomic models of the A and B states of EGFP and E^2GFP obtained by point mutation of the known crystal structures of homologous variants. The B states of S65T and WT were also simulated for comparison. The Amber98 force field[13] was used, and the parameters for anionic and neutral chromophore configurations were derived. EGFP was chosen as a "prototype" for variants with a stabilized anionic chromophore. In E^2GFP the neutral chromophore is instead more stable, as in WT GFP. However, state A of E^2GFP is almost completely nonfluorescent pointing to the existence of an efficient nonradiative channel for de-excitation.[11,12] Though this behavior may seem unfavorable for biological application, a very promising property was shown for this mutant, namely a light-induced on/off switching between long-lived (>5 min) bright and dark states.[14] Other yellow GFP variants display a similar behavior: the single-molecule experiments by Dickson et al.[15] showed that the fluorescence of S65G/S72A/T203Y and S65G/S72A/T203F mutants could be recovered by some minutes of irradiation at 400nm (i.e., in the neutral-state absorption band).[15] E^2GFP was instead found to recover after few seconds of UV illumination (at 350 nm), thereby suggesting the existence of a dark state distinct from the states populated at equilibrium.[14]

WT GFP in the A state was already investigated by molecular dynamics simulations, which pointed out the rigidity of the fold of the protein and the stability of the H-bond network surrounding the chromophore.[16] A parameterization of the CHARMM-like force field for the neutral and anionic chromophore was provided in Ref. 17, together with a molecular dynamics simulation of the S65T mutant, which questions the protonation of Glu222 in state B. Our study is aimed at monitoring the structural rearrangements induced by the mutations around the chromophore and the consequent changes in the H-bond network, which determines the equilibrium between the anionic and neutral forms of the chromophore and the pathways of possible proton transfers. Those are relevant because they drive the transition between equilibrium A and B states and other nonfluorescent states involved in the fluorescence dynamics of GFPs. Indeed, fluorescence correlation spectroscopy[18,19] and single-molecule experiment[15,20,21] revealed flickering and blinking events that are attributed to changes in the protonation form of the chromophore, such as anionic/zwitterionic or anionic/neutral state transitions.

The article is organized as follows: a detailed description of the starting structures is reported in Methods, together with the derivation of the force field parameters of the chromophore and the protocol used in the molecular dynamics simulations. The results of the MD simulations are summarized, starting from a comparison between the MD average structures and the X-ray structures of various mutants, in order to highlight the structural changes induced by the mutations. The different dynamical features are addressed by monitoring the network of H-bonds during the simulations. Finally, the output of this MD study in the understanding of GFP photophysics is discussed.

METHODS

Homology Modeling

The starting structures of EGFP (S65T/F64L) and E^2GFP (S65T/F64L/T203Y) with the chromophore in the neutral and anionic forms were modeled from X-ray structures of other mutants, using the InsightII software.[22] The simulation of the S65T mutant started from its X-ray structure,[6]

TABLE I. Description of the Starting Homology Modeled Structures: The PDB Code of Each Fragment

	Main chain	Chromophore	F64	T/Y 203	H148	E222	Water molecules
$EGFP_A$	1emb	1emb	1emca	1emb	1emb	1emb	1emb
$EGFP_B$	1emg	1emg	1emca	1emg	1emg	1emg	1emb
E^2GFP_A	1emb	1emb	1emca	2yfp	1emb	2yfp	2yfp
E^2GFP_B	1emg	1emg	1emca	1yfp	1yfp	1yfp	2yfp

with Protein Databank[23] (PDB) code 1emg. The starting structure of WT in the B state was modeled from 1emg. The methyl group of Thr65 was substituted by a hydrogen atom, and the resulting Ser65 side chain was flipped to the same configuration present in the A state of WT.

Table I summarizes how each model was built starting from fragments belonging to different X-ray structures. The main chain of the B state (with the anionic chromophore) of EGFP and E^2GFP was taken from 1emg. The choice of this particular structure was made on the basis of its lowest average root mean square distance (RMSD) fitted to the α-carbons (Cα) atoms from the other PDB structures assigned to state B, including 1ema[2] (with mutation S65T), 1emk[5] (S65C,F64L,I167T,K238N), and 1yfp[10] (S65G,V68L,S72A,T203Y). The main chain of the A states was instead modeled from the 1emb PDB structure of wild-type GFP. This structure was chosen because it has the lowest Cα RMSD from 2yfp[10] (S65G,V68L,S72A, H148G,T203Y), which can be assigned to state A (see below) and has the T203Y mutation like E^2GFP. Y203 was modeled from structures 1yfp and 2yfp. Because of the S65G mutation, 1yfp is mainly found in the B state,[10] whereas the additional H148G mutation of 2yfp favors to a certain extent the neutral form (state A). The positions of Y203 and E222 in the A and B states of E^2GFP were thus taken from 2yfp and 1yfp, respectively. As is the case for WT and S65T, the configuration of T203 was taken to be different in the A and B states of EGFP. Although the hydroxyl group of T203 points toward the chromophore in the B state, the side chain is flipped in the A state, as revealed by spectroscopy experiments.[4] The F64L mutation is present in both EGFP and E^2GFP and was taken in all cases from 1emc[5] (chain A).

There are several water molecules inside the protein, their number differing within the set of PDB structures. The largest number of internal water molecules is present in the structure 1ema, which was thus chosen to model the internal solvent molecules of EGFP in states A and B. Concerning E^2GFP, the water molecules of 2yfp were used, few of them being absent in 1yfp. Two other water molecules are missing in 2yfp (W320 and W383 of 1ema), although there is no local change in the sequence to justify their absence. Thus, they were added to the structure.

The addition of missing side-chain and hydrogen atoms was performed by the Leap program of the Amber suite.[13] The protonation of the eight histidine residues was inferred from the presence of hydrogen donor or acceptors in the surroundings of their imidazole group. Histidine residues at positions 25, 148, 181, 199, and 217 were protonated at their δ nitrogen atom (N_δ), while those numbered 81 and 139 were protonated at their ε nitrogen atom (N_ε). However, in the case of residues 77 and 169 the protonation could not be unambiguously determined, because their immediate environment is constituted by water molecules the orientation of which cannot be established from the X-ray structures. Histidine 77 is solvent exposed and its protonation does not influence the H-bond network in the inside of the protein. Following Ref. 16 its imidazole group was protonated at N_ε. Residue 169 is instead located inside the β-can and may influence the bond network surrounding the chromophore. Following Ref. 16 we protonated its N_ε. As is the most accepted picture, we chose to protonate the carboxylic group of Glu222 in state B and leave a carboxylate in state A. The different protonation of Glu222 in states A and B is debated, because the feature corresponding to this change is absent in the FTIR (fourier transform infrared spectroscopy) difference spectrum.[24] However, a theoretical calculation of the vibrational spectra suggested that this feature may be obscured because of the presence of a carbonyl mode in the imidazole ring of the neutral chromophore.[25] The remarkably good agreement between our MD simulation and the X-ray structure of S65T supports the protonation of Glu222 in the B state.

Each system was neutralized by the addition of 6 Na^+ ions and solvated in a box of tip3 water molecules, each side of the protein being kept 8 Å apart from the box boundary. In numbers, about 8800 water molecules (beyond those from homology modeling) were added to the structures, and the resulting box dimensions were approximately $63 \times 77 \times 78$Å, with a total of about 30,000 atoms.

Force Field Parameters for the Chromophore

The parameters for the chromophore derived in Ref. 17 are consistent with the CHARMM force field.[26] Here we used the Amber98 force field,[13] and the parameterization of the chromophore (shown in Fig. 1) was done accordingly. The equilibrium bond lengths, angles, and dihedrals were taken from ab initio DFT optimized structures of a neutral and anionic model chromophore, consisting of the two aromatic rings linked by the bridging carbon and two methyl groups substituting the linkage of the chromophore to the protein. The same models were used to derive the partial charges (reported in Fig. 1), by means of a standard procedure consisting in the fit of the electrostatic potential computed at the HF/6-31G* level.[27] The charges of the Gly67, Thr65, and Ser65 fragments linking the chromophore to the protein backbone were those of Amber98. The covalent force constants and van der Waals parameters were assigned in analogy with Amber98.

Simulation Protocol

We followed the standard protocol for a MD simulation, which consists of an initial minimization, followed by gradual heating of the system. The solute is initially minimized by 1000 steps of steepest descent and conjugate gradient, and then the water is equilibrated around the solute with 20 ps of molecular dynamics, keeping a constant temperature of 298K and pressure of 1 atm (Berendsen algorithm), in order to obtain the correct water density. The whole system is then minimized at constant volume for about 1000 steps. The heating procedure starts with 10 ps of MD at 50K, followed by 20 ps at 150K and 30 ps at 298K. The gradual increase of temperature is needed to obtain an even distribution of energy between degrees of freedom. The production run follows, for about 800 ps–1 ns. The particle-mesh-Ewald method was used to calculate nonbonded interactions (i.e., van der Waals and electrostatic), while SHAKE was applied to bonds involving hydrogen atoms allowing a 2 fs time-step. Within an MD trajectory the coordinates were dumped every 1 ps.

Free Energy Calculations

Differences between the free energy of state A and state B of EGFP and E^{2}GFP were calculated using the thermodynamic integration (TI) procedure (for a review of free energy calculation techniques see Ref. 28). Denoting with U_A and U_B the potential energies of state A and B, respectively, intermediate nonphysical states are defined by the following expression for the potential energy:

$$U_\lambda = (1-\lambda)U_B - \lambda U_A, \quad 0 \le \lambda \le 1\,. \tag{1}$$

The parameter λ describes the level of (linear) mixing between the initial (B) and final (A) state. In the present case U_λ only contains contribution from the chromophore and Glu222, which in our model change protonation in going from the B to the A state. The change in free energy can then be calculated as

$$\Delta G_{AB} = G_A - G_B = \int_0^1 \langle \partial U/\partial\lambda \rangle d\lambda\,, \tag{2}$$

where $\langle \cdots \rangle$ denotes the ensemble average. The integral in the latter equation is approximated by a gaussian quadrature formula

$$\Delta G = \sum_{i=1}^{n} w_i \langle \partial U/\partial\lambda \rangle_{\lambda_i}\,, \tag{3}$$

where λ_i's are the quadrature points and w_i's the corresponding weights. Within this framework, we performed five 150-ps simulations (plus 50 ps of initial equilibration) for each of the two mutants at λ = 0.04691, 0.23076, 0.50000, 0.76923, 0.95308 and calculated the sum in Equation 3 with the appropriate gaussian weights w_i's. Representative structures of the B state of E^{2}GFP and EGFP were taken as starting structures, and the protocol applied for the molecular dynamics was the same as that for the 1-ns simulations. The statistical errors over the calculation of the derivative in Equation 3 were estimated by dividing each 150-ps simulation in 15 contiguous bins of 10 ps and taking the average within each bin. The error over the free-energy result was evaluated as the standard deviation within the set of the 15 averages.

States A and B of EGFP differ also in the conformation of Thr203 and the two configurations of Thr203 cannot be simultaneously explored in a 150-ps simulation because of the high-energy barrier between the flipped and unflipped Thr203 geometry. Thus, in principle, a sampling of this structural difference should be implemented in the hamiltonian. However, a test over some values of λ showed that the difference between the calculation of the flipped and unflipped Thr203 is within the statistical error.

We finally observe that it is possible to use the linear mixing in Equation 1 since the "appearing" and "disappearing" atoms (i.e., the hydrogen atom of the chromophore phenol group and the one on Glu222-COOH, respectively) have no VdW terms, as is the case for all oxygen bound hydrogen atoms in the Amber force field. Otherwise special care would be required for the treatment of the divergency of the integral at $\lambda = 1$ and $\lambda = 0$.[28]

RESULTS

Comparison with Crystal Structures

We performed molecular dynamics simulations starting from the models described in the previous section, namely E^{2}GFP and EGFP both in the A and B states, and the B state of WT GFP. As a test system, we also simulated the S65T mutant in the B state, whose structure is known from X-ray crystallography,[6] in order to better discern the influences of the mutations and prove the goodness of the force field for the chromophore. Figure 2 shows the root means square deviations (RMSDs) of the S65T trajectory from the X-ray structure 1emg and of EGFP$_B$ from the starting structure. The various RMSDs shown are fitted to the α-carbons (Cα), to heavy atoms, to residues inside the β-can and to the environment of the chromophore. The average Cα RMSD during the simulation is 0.75 Å in S65T and 0.70 Å in EGFP$_B$, the same order as found in the simulation of wild type GFP (WT).[16] The heavy atom RSMD average is larger (1.15–1.25 Å) because of the presence of flexible loops and turns and solvent exposed residues. When only the residues inside the β-can are taken into account, the average RMSD decreases to 0.72 Å in S65T and to a slightly larger value (0.86 Å) in EGFP$_B$. If only the environment of the chromophore is considered the RMSD drops to 0.53 Å in S65T (0.64 Å in EGFP$_B$), revealing a remarkable stability. The larger values of internal and environment RMSDs in EGFP$_B$ are due to the presence of mutated residues, which produce some rearrangements with respect to the starting structure (see below). The other simulations show similar RMSD behaviors.

The internal dynamics of wild-type GFP (WT) was described by McCammon et al.[16] with an MD study. Here the interest is focused on the effects of mutations in the chromophore environment. In order to analyze the structural differences we computed the average structures

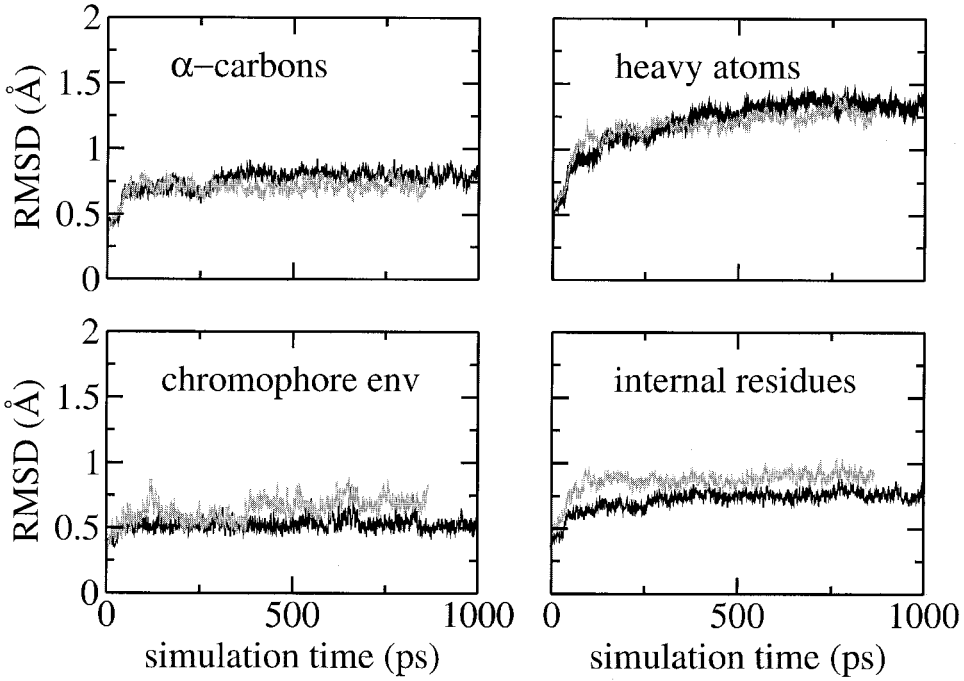

Fig. 2. Root mean square distance from the crystal structure (1emg) during the simulation of the S65T mutant (dark lines) and $EGFP_B$ (light lines), fitted to the α carbons (top left), heavy atoms (top right), chromophore environment, i.e., residues 64–69, 94, 145, 148, 165, 167, 183, 203, 205, 222, W1–W6 (bottom left), and residues inside the β-can, i.e., 2, 4, 8, 10, 12, 14, 16, 18, 20, 22, 27, 29, 31, 33, 35, 37, 40, 42, 44, 46, 48, 53–72, 74, 78, 81–87, 91, 92, 94, 96, 98, 100, 103, 104, 106, 108, 110, 112, 119, 121, 123, 125, 127, 129, 130, 136, 141, 145, 148, 150, 152, 161, 163, 165, 167, 169, 177, 179, 181, 183, 185, 187, 193, 196, 199, 201, 203, 206, 207, 209, 217, 218, 220, 222, 224, 226 (bottom right).

during the trajectories and compared the resulting chromophore environment configurations with the X-ray structures. As shown in Figure 3(a), there is a good superposition between the MD average and the X-ray structure of the S65T mutant, which validates the force field parameters used in the present calculations. The B state of WT, superimposed in Figure 3(b) with the X-ray structure of S65T, shows a different orientation of Glu222, resulting in a H-bond to Ser205 which is absent in S65T. This feature, discussed below in more detail, is not present in the proposed models for the B state of WT GFP.[4]

The averaged structures of EGFP and E^2GFP are superimposed in Figure 3(c,d) with the X-ray structures of WT (A states) and S65T (B states), respectively. A shift of the position of the chromophore is observed in EGFP and E^2GFP because of the F64L mutation, which pulls the chromophore in order to accommodate the isopropyl group of Leu64 in the place of the phenyl of Phe64. This can be also observed comparing WT (PDB code 1ema) with the F64L variant (1emm[5]). The surrounding residues (Gln94, Arg96, His148, Glu222) move accordingly, in order to maintain the H-bond interactions with the chromophore. In $EGFP_A$ and E^2GFP_A, the orientation of Glu222 changes with respect to that in WT as a result of the S65T mutation, which imposes a different geometry of the Thr65-OH·Glu-COO^- H-bond. Apart from the configuration of water molecules, the structures of EGFP and E^2GFP are similar. A small difference is present in the B state of E^2GFP, where Glu222 moves nearer to its H-bond donor W4, as a consequence of the absence of W3.

Figure 3(e,f) shows the structural differences between state A and B within the same GFP variant. In $EGFP_A$ and—to a minor extent—in E^2GFP_A, the phenolic ring of the neutral chromophore is pushed backwards (in the y direction) as a consequence of the rearrangement of hydrogen atoms. Moreover, the carboxyl group of Glu222 changes orientation, being almost perpendicular to the plane of the chromophore in the B states and nearer to it in the A states. Those same structural differences are observed when comparing the crystal structures of WT (mainly in state A) and S65T (mainly in state B), though the rotation of Glu222 is less pronounced [see Fig. 3(c)]. In E^2GFP_A, the Tyr203 phenol undergoes a parallel shift due to a rearrangement of W4, W5, and W6, which takes place within the first 20 ps of simulation of the A state. The different orientation of Thr203 side chain in EGFP [Fig. 3(e)], which was already included in the starting models, is a characteristic structural difference between the A and B state of WT[4] and possibly of other GFP variants with Thr203. Models of state I, which is the result of the excited state proton transfer from A, suppose the same orientation of Thr203 as in the A state, but with an anionic chromophore.

Hydrogen Bond Network

Though the average structures measure the atom displacements due to mutations, they give an incomplete

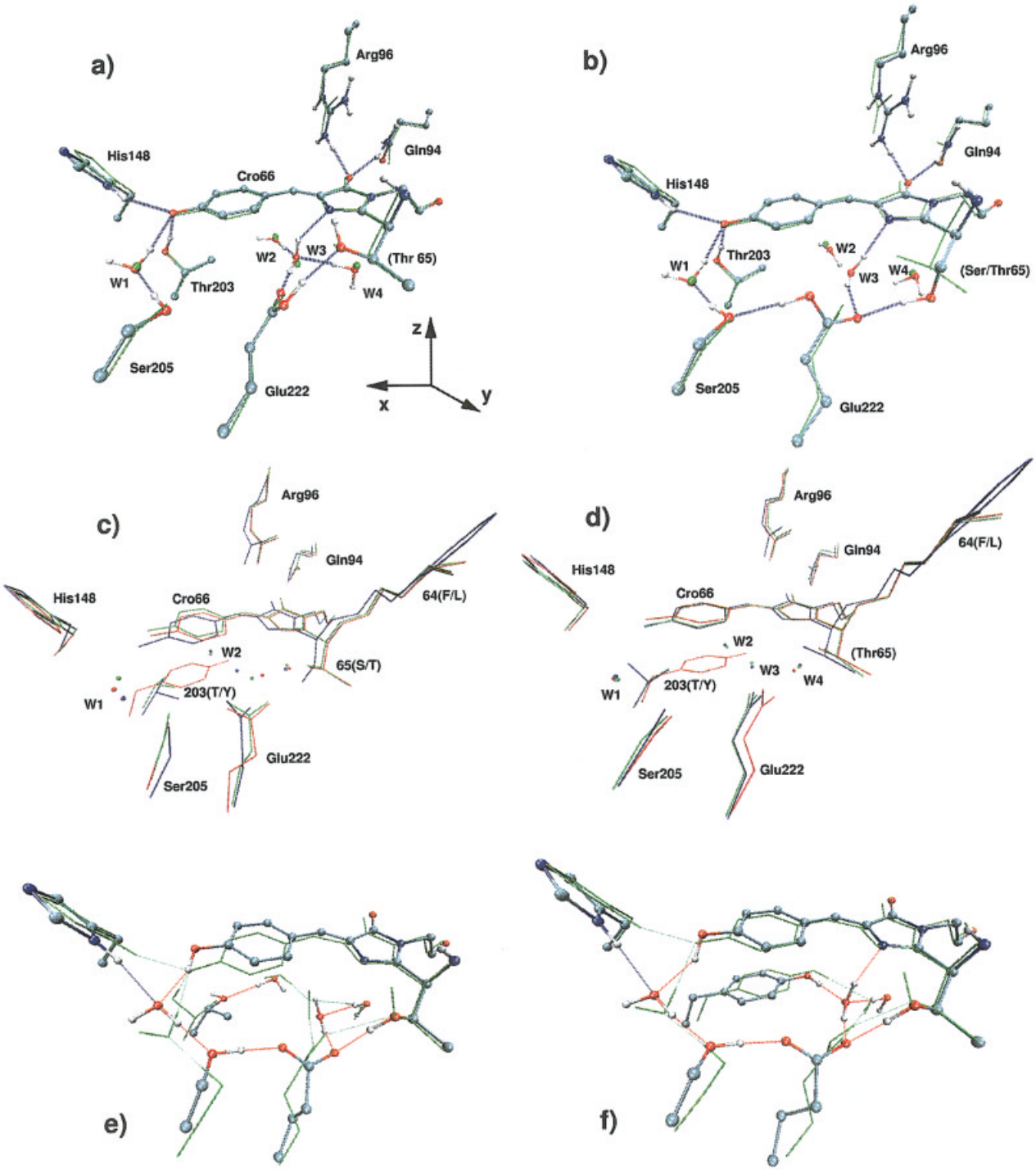

Fig. 3. (a) Comparison between the X-ray structure of the S65T GFP mutant (in green) and the 100-step-minimized time-averaged structure resulting from the simulation (color code for atoms, i.e., red for oxygen, blue for nitrogen, white for hydrogen, and cyan for carbon). Only polar hydrogen atoms are shown. (b) Comparison between the X-ray structure of the S65T GFP mutant (green) and the average structure of WT GFP_B resulting from the simulation. (c) Comparison between the crystal structure of WT (PDB code 1ema) (blue) and the minimized average MD structures of $EGFP_A$ (green) and E^2GFP_A (red). Hydrogen atoms are not shown. (d) Comparison between the MD minimized structures of the B states of S65T (blue), EGFP (green), and E^2GFP (red). (e) Comparison between the minimized average MD structures of $EGFP_A$ (atom code color) and $EGFP_B$ (in green). Only polar hydrogen are shown. (f) The same as (e) for the E^2GFP mutant. All structures are superimposed on the Cα. The figure was produced with VMD.[29]

representation of the configurations explored during the dynamics, and in particular they do not account for the different strength of H-bonds. Figure 4 shows the H-bonding network occupancy around the chromophore monitored during the MD simulations. Apart from the weak interaction between Glu222 and Ser205, the H-bond net-

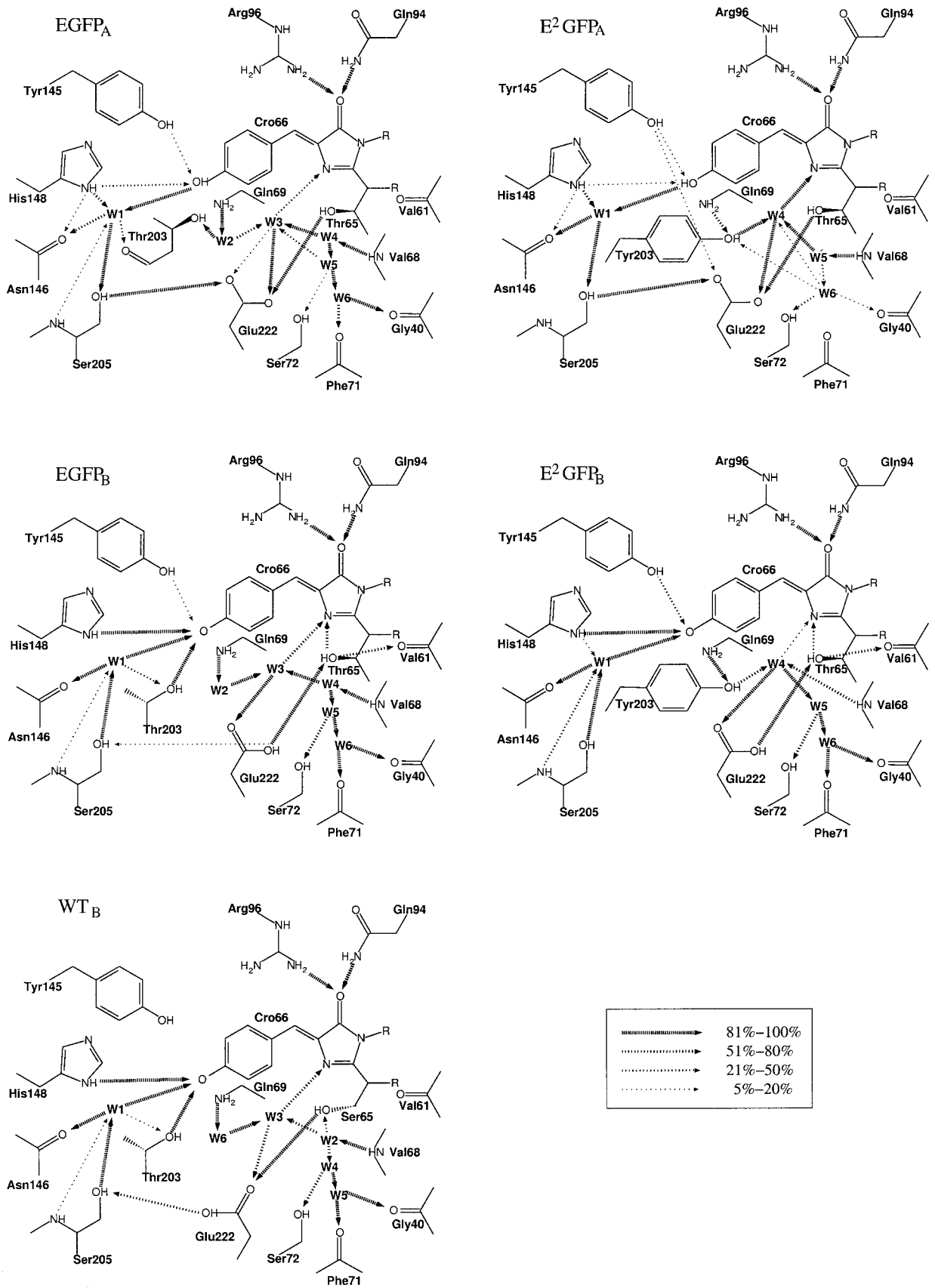

Fig. 4. H-bond network around the chromophore in the A and B states of EGFP and E^{2}GFP, and in the B state of WT GFP. The varying width and density of the arrows indicate a different occupation of the H-bond during the trajectory. An H-bond was considered as occupied when the donor-acceptor distance was <3.5 Å and the donor-hydrogen-acceptor angle $<40°$.

work of S65T in state B is the same as that of $EGFP_B$ and is not reported in Figure 4.

As in WT,[16] A states are characterized by a stable H-bond chain connecting the phenol of the Cro66 to the carboxylate of Glu222 through W1 and Ser205. The presence of this H-bond chain, which in WT provides the path for the proton leaving the excited chromophore, indicates that other phenomena rather than its perturbation are responsible for the suppression of the excited state proton transfer in EGFP and E^2GFP. The interactions of W1, however, are different from WT. The medium-strength (75%) interaction with the imidazolidinone of His148 is absent in WT,[16] and the H-bond with the carboxyl group of Asn144 backbone has a lower occupation (38% in WT vs. 75% in $EGFP_A$ 95% in E^2GFP_A).

The network involving W2-W6 in $EGFP_A$ is similar to WTs. Indeed, the only difference in this region is the methyl of Thr65, which is absent in Ser65 of WT. This mutation changes the geometry of the H-bond involving Thr65 and Glu222, and consequently perturbs the interactions of W3 and W4. In particular, the H-bond between W3 and the nitrogen in the imidazolidinone of the chromophore (N2 in Fig. 1) is weaker (77% in WT vs. 30% in $EGFP_A$).

Regarding E^2GFP_A, with respect to the starting structure, there is a movement of the water molecules below the imidazolidinone of the chromophore (W4,W5, and W6). Thanks to the space left available by the rotation of Glu222 [see Fig. 3(c)], W4 moves closer to the imidazole ring of the chromophore, forming a stable H-bond with N2 (80% in E^2GFP_A vs. 30% of W3 in $EGFP_A$). W5 takes the place left by W4 and in turn W6 moves in W5's former position. Upon this rearrangement, W6 is less stable, its average fluctuation amounting to 1 Å in contrast to the 0.5 Å value in E^2GFP_B.

An additional feature is present in E^2GFP_A, i.e., the weak bond between the hydroxyl group of Tyr145 and the carboxylate of Glu222. This bond is formed during the simulation for about 50 ps, thanks to a rearrangement of Tyr145. In particular, the distance between the hydroxyl group of Tyr145 and the oxygen of Glu222 shortens to <3 Å from a value >5 Å during the rest of the simulation. This new configuration of Tyr145 involves only minor displacements of the surrounding residues.

A key difference between $EGFP_B$ and E^2GFP_B is the absence of the Thr203 hydroxyl donor. The H-bond with Tyr145 is stronger in E^2GFP than in EGFP (35 vs. 5%), and the average distance between Tyr145 donor and Cro66 acceptor is shorter (3.65 vs. 4.26 Å in EGFP and a value between 4.50 and 4.60 Å in the crystal structures). Despite this, the phenolate is altogether less well coordinated in E^2GFP_B, owing to the absence of the strong interaction with Thr203-OH. Also the imidazolidinone nitrogen (N2) is less coordinated in E^2GFP_B. Indeed, the medium-strength (60%) H-bond between W3 and N2 in $EGFP_B$ is replaced by a weak interaction (5%) between N2 and W4 in E^2GFP_B.

The Glu222-COOH·Ser205-OH H-bond is very weakly occupied (5%) in $EGFP_B$, and with opposite direction respect to the A states. When this bond is occupied, the H_δ of Glu222 rotates from an *syn* to a *anti* position. This shows that it is possible to cross the *syn-anti* energy barrier thanks to favorable fluctuations of the environment. The same feature is absent in the simulations of E^2GFP_B and S65T, probably owing to the limited exploration of the phase space. In contrast to our results, a previous MD study of S65T [17] found a stable Glu222-COOH·Ser205-OH H-bond, which resulted in a distorted geometry of Glu222 with respect to the X-ray structure. We believe that the simulation reported in Ref. 17 preferably explored a configuration with an *anti* rotated H_δ of Glu222, which is only scarcely accessed in our trajectory.

The H-bond network of WT in the B state is similar to that of $EGFP_B$ near the chromophore phenolate, whereas it mainly differs in Glu222 orientation. The absence of Thr65 methyl group results in a configuration which allows Ser65-OH to donate a H-bond to Glu222-COOH. This new configuration brings Glu222 closer to Ser205-OH and favors the Glu222-COOH·Ser205-OH H-bond, which involves an *anti* configuration of the H_δ of Glu222. As shown in Figure 5, the *syn* configuration of Glu222-COOH is also occupied during the simulation, reducing the population of the Glu222-COOH·Ser205-OH H-bond to 63%. According to our results, the model for the B state of WT proposed in Ref. 4, which included only the *syn* isomer of Glu222-COOH, should be extended to include the different orientations of Glu222. Scharnagl et al.[30] reported a 3.1 k_BT preference in the free energy of the *syn* over the *anti* isomer of Glu222 in the chromophore environment. The calculation in Ref. 30, however, does not account for the flexibility of the side chain of Glu222, thereby excluding the possibility that a more favorable orientation of Glu222 could farther reduce the energy difference between the *syn* and *anti* substates, and allow the population of the *anti* configuration.

Some residues of the chromophore environment are partially solvent exposed. For instance, the deprotonated nitrogen of His148 imidazole ring is accessed by a water molecule outside the protein fold. In addition, W1 is close to the surface of the protein. However, only one H-bond compatible configuration between W1 and an external water molecule could be found over 0.9 ns of MD simulation and only in $EGFP_B$. In the case of $EGFP_A$ a water oxygen gets close to W1 (distance <3.5 Å) but the donor-hydrogen-acceptor angle is too large ($>60°$) for a H-bond. None of the simulation performed showed a direct contact of the chromophore with an external water molecule.

Flipped Thr65 Side Chain

During the simulations of the A states the side chain of Thr65 flips from a configuration in which it is H-bonded to Glu222 to one in which it contacts the backbone oxygen of Val61 and of Leu64. These H-bonds are not very stable, however, and their overall occupation is small ($\sim$5%). Still, the time during which the Thr65 side chain is flipped amounts to about 15–20% of the total simulation time, and consequently the Thr65-OH·Glu222-COO^- H-bond is weakened, its occupation being $\sim$85% in E^2GFP_A and $EGFP_A$ in

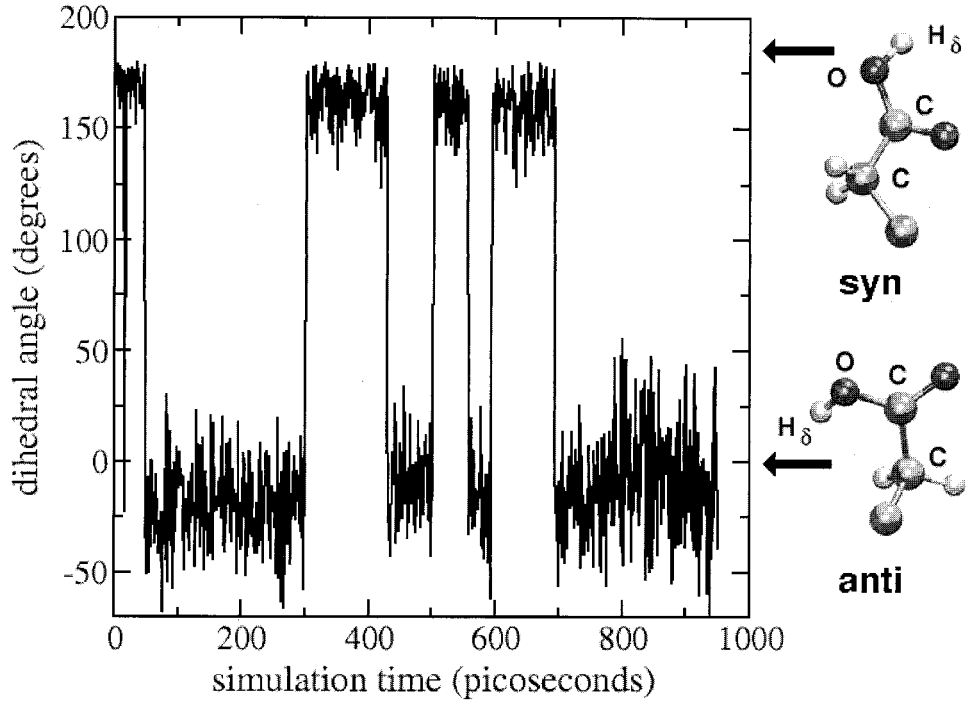

Fig. 5. C–C–O–H dihedral angle of Glu222 during the simulation of WT_B. The configurations corresponding to *syn* and *anti* positions of the H_δ are shown in ball-and-stick.

contrast with the 100% of WT.[16] This is rather unexpected, because the negative charge of Glu222-COO^- should attract the polar hydroxyl group of Thr65. However, apart from the charged Glu222, the Thr65 side chain is surrounded by several nonpolar residues such as Leu42, Leu44, Phe46, Val61, Val68, Leu220, which make favorable van der Waals (VdW) interactions with the Thr65 methyl group. To investigate the energetics of the flipping, we calculated the energy of Thr65 side chain as a function of the dihedral angle around the Cβ–Cα bond and reported the results in Figure 6. The curves were obtained by dihedral rotating the Thr65 side chain of the minimized average structure of E^2GFP_A from 0° to 360°, with a step of 10°. The hydrogen atoms of Thr65 and the surrounding residues of each resulting structure were minimized (500 steps of minimization), and the energy was calculated as the difference between the total energy of the protein and the energy of the protein without the Thr65 side chain (containing Cα, Cβ, the methyl group, and the hydroxyl group). The filled squares in the figure represent the same quantity calculated during the MD simulation. The same calculation for $EGFP_A$ gave very similar results not reported here. The region at 290° (i.e., −70°) is mainly occupied during the simulation and corresponds to the minimum of the energy, whereas the shallow region of the flipped chromophore (at 180°) is less populated. The third minimum is well separated by high-energy barriers and is seemingly not relevant. The presence of the shallow region is due to an interplay between VdW and electrostatic interactions. Although the minimum electrostatic interactions are reached with the shortest Thr65-OH·Glu222-COO^- distance, the VdW component has a rather constant

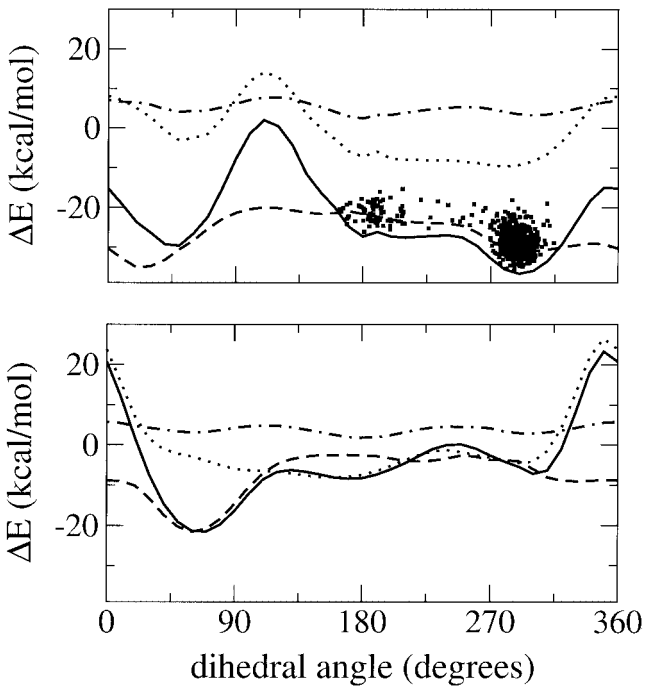

Fig. 6. Top: Energy (solid line) of Thr65 as a function of the dihedral angle (OG1-CG1-CA1-C1), calculated as the difference between the total energy of the protein (E^2GFP_A) and the energy of the protein without Thr65. The VdW (dotted line), electrostatic (dashed), and covalent (dotted-dashed line) components are shown. The filled squares are the values of the energy calculated during the MD trajectory. Bottom: same as top panel for Ser65 of WT_A.

behavior in the region between 200° and 300° and accounts for the high-energy barrier separating the two populated configurations from the third one. A similar calculation for WT (bottom panel of Fig. 6) shows again a deep minimum (~70°, corresponding to the Ser-OH·Glu222-COO$^-$ H-bond) and a shallower one (~180°). Although the electrostatic and covalent components are similar to those of EGFP and E^{2}GFP, the VdW part accounts for the different behavior of the curve, as a consequence of the methyl substituent present in threonine. In the case of WT the energy barrier between these two states is higher (15 vs. 10 kcal/mol in the S65T mutants), and consequently the region corresponding to the flipped Ser65 is not populated at room temperature.[16] These results rationalize why the Thr65-OH·Glu222-COO$^-$ H-bond is less stable in the A states of S65T mutants.

Free Energy Calculations

To investigate the energetics of proton equilibrium, we calculated the free energy difference between state A and B (ΔG_{AB}) in EGFP and E^{2}GFP at neutral pH (i.e., with protonation of amino acids corresponding to pH 7). The two states differ in the protonation form of the chromophore and of Glu222, and their free energy contains terms of internal strain (bond, angle, and dihedral), which change accordingly. Because the classical force field hamiltonian cannot correctly describe energy differences between covalent structures, the meaningful value is not the ΔG_{AB} by itself but rather the difference between the two mutants (i.e., $\Delta G_{AB}^{EGFP} - \Delta G_{AB}^{E^2GFP}$). Indeed the internal contributions are the same in the two mutants and cancel out in the difference. From the resulting values of ΔG_{AB} (17.3 ± 1.2 kcal/mol in E^{2}GFP and 23.1 ± 2.6 kcal/mol in EGFP) we get $\Delta\Delta G_{AB} = \Delta G_{AB}^{EGFP} - \Delta G_{AB}^{E^2GFP} = 5.8 \pm 2.8$ kcal/mol.

We can derive the experimental $\Delta\Delta G_{AB}$ from absorption measurements of the two GFP variants:

$$\Delta\Delta G_{AB} = \Delta G_{AB}^{EGFP} - \Delta G_{AB}^{E^2GFP} = -\frac{1}{k_B T} \ln \frac{R^{EGFP}}{R^{E^2GFP}}, \qquad (4)$$

where $R = n_A/n_B$ is the ratio between the population of state A and state B at neutral pH. These populations can be estimated by a deconvolution of the absorption spectra.[12,31,32] Owing to the presence of the ratio R^{EGFP}/R^{E^2GFP}, we do not need to take care of the different cross section of states A and B. Indeed it can be assumed than only irrelevant variations of the cross section occur for the same protonation state of the chromophore in the two variants. From these considerations we get $R^{EGFP}/R^{E^2GFP} = 0.08 \pm 0.03$, which leads to $\Delta\Delta G_{AB} = 5.0 \pm 0.8$ kcal/mol. Despite a quite large statistical error, the theoretical $\Delta\Delta G_{AB}$ value agrees fairly well with that derived from the absorption spectra.

DISCUSSION

The main objective of this study is the investigation of the structural and dynamical modifications induced by mutations F64L, S65T, and T203Y in GFP. The F64L mutation is known to improve folding efficiency.[9] In the folded protein its only effect is a shift in the position of the chromophore. The effects of the S65T mutation are more relevant: it destabilizes the neutral chromophore in favor of the anion.[2] Because in the A state the chromophore is neutral and Glu222 is anionic, H-bond donors to Glu222 are crucial in stabilizing its negative charge. It was proposed that Thr at position 65 cannot adopt a correct conformation for donating a H-bond to Glu222.[9] Here we provide a different explanation. In fact, in our simulations we observe a rather stable Thr65-OH · Glu222-COO$^-$ H-bond in E^{2}GFP$_A$ and EGFP$_A$ consistently with the fact that state A is predominant in E^{2}GFP and that the population of state A in EGFP is sizable.[12] However, this bond is less stable than in WT, because of the presence of a configuration with a flipped Thr65 side chain, in which Thr65-OH is too far away from Glu222-COO$^-$ to form a H-bond. Thus, the S65T mutation reduces the population of state A in EGFP (and in the S65T mutant), because it partially destabilizes the Thr65-OH · Glu222-COO$^-$ H-bond. State A is completely suppressed either when this H-bond is missing, like in S65G mutants, or when the B state is additionally stabilized, like in the Emerald variant, in which the I167T mutation provides an additional H-bond to the anionic phenolate of the chromophore.[33]

The additional T203Y mutation in E^{2}GFP restores an equilibrium between state A and B similar to that of WT, i.e., with a predominant A state.[12] Rather than favoring the neutral state of the chromophore, Tyr203 destabilizes the anion, because it subtracts a H-bond donor—namely the hydroxyl group of Thr203—to the phenolate of the chromophore. The simulation of E^{2}GFP$_B$ shows that the H-bond with the close phenolic group of Tyr145 is not stable, because it involves a distortion of the chromophore planarity. Indeed the force field models the tendency of the chromophore to remain planar, at least in the anionic form. Though, as said before, the equilibrium population of state A and B of E^{2}GFP resembles that of WT, both states are—to a certain extent—destabilized in E^{2}GFP, pointing to a lower ground-state energy barrier among them.

These structural considerations are supported by a comparison of the free energy of states A and B in EGFP and E^{2}GFP. The agreement of our free energy calculation with the experimentally derived value supports our structural models for A and B states of EGFP and E^{2}GFP and reflects the accurate description of the nonbonded interactions, and in particular of the electrostatic part, which is the determining contribution to the equilibrium between the two states.

States A and B do not embody the whole photophysics of GFP mutants. Fluorescence dynamics and single-molecule studies suggest the existence of dark states, from which the bright state can be recovered either spontaneously, as in blinking/flickering,[15,18] or after blue or UV light irradiation, as in the on/off switching.[15,14] Blinking may involve a transition from an anionic to a zwitterionic form of the chromophore, the latter being dark due to an efficient path of radiationless decay through photoisomerization.[7] Because the zwitterion is protonated in the imidazolidinone nitrogen (N2), it is interesting to evaluate possible donors to N2. From our simulations, one possible protonation

path goes from Glu222-OH to N2 through the medium strength (occupation 45/55%) H-bond between Thr65-OH and N2. In this configuration Glu222 donates the proton and is left with a negative charge as in the A state. Another possible proton donor is the water molecule below N2, which forms a rather stable H-bond in EGFP (occupation 70%) and a much weaker one in E^2GFP. The resulting OH^- anion could be stabilized by a net of H-bonds involving W2 (T203 in E^2GFP) and Gln69.

The flickering revealed in fluorescence correlation spectroscopy experiments[18,19,34] is instead interpreted as a fast (tens of μs) transition between neutral and anionic forms of the chromophore. The rate of one flickering component was found to be pH dependent in EGFP, suggesting a proton exchange with the bulk solvent.[18] One H-bond compatible configuration of W1 (the water molecule H-bonded to the phenolate of Cro66) with external water molecules is found in our 0.8-ns simulation of EGFP. Though rare events in the nanosecond time scale, these H-bonds can make the chromophore sensitive to the external proton concentration, as proposed in Ref. 18 and influence the rate of dark- to bright-state transition.

CONCLUSIONS

By means of molecular dynamics simulations we studied the A and B states of EGFP (F64L/S65T) and E^2GFP (F64L/S65T/T203Y) and the B states of S65T and WT GFP. Structural differences between these mutants were reported, together with H-bond networks around the chromophore. In contrast with the results of Ref. 17, our study supports the protonation of Glu222 in the B state, as shown by the good agreement with the starting structure in the S65T simulation. Additionally, a free energy calculation of the relative stability of state A with respect to this model of the B state (i.e., with a protonated Glu222) correctly reproduces the change in the equilibrium between these two states from EGFP to E^2GFP as detected by absorption measurements.

Moreover, our simulation of WT in the B state showed that both *syn* and *anti* isomers of Glu222-COOH are occupied, extending the previous model in which a single orientation of Glu222 was considered, i.e. the same as in S65T. Finally, a mechanism for destabilization of the neutral chromophore in S65T mutants was proposed, based on the sizable population of a flipped-Thr65 configuration that weakens the H-bond with Glu222-COO^-, necessary to stabilize the negative charge of the carboxylate.

Our study also provides the starting point for characterization of the dark states involved in the photodynamical behavior of EGFP and E^2GFP. In the hypothesis that a transition to a zwitterionic chromophore is responsible for the blinking of single EGFP molecules, it would be interesting to study the dynamics of the proton transfer connecting the anionic to the zwitterionic form of the chromophore. By our MD study, we were able to suggest possible proton transfer pathways for such transition. Finally, the mechanism underlying the light-controlled on/off switching of E^2GFP also needs to be identified. Structural changes, among which the most promising seem to be *cis-trans* photoisomerization of the chromophore, are being investigated as those leading to the reactivable dark state.

ACKNOWLEDGMENTS

We thank Fabio Beltram and Teodoro Laino for helpful discussions and suggestions. We acknowledge the allocation of computer resources from INFM Progetto Calcolo Parallelo.

REFERENCES

1. Cubitt AB, Heim R, Adams SR, Boyd AE, Gross LA, Tsien RY. Understanding, improving and using Green Fluorescent Proteins. Trends Biochem Sci 1995;20:448–455.
2. Ormö M, Cubitt AB, Kallio K, Gross LA, Tsien RY, Remington SJ. Crystal structure of the Aequorea Victoria Green Fluorescent Protein. Science 1996;273:1392–1395.
3. Yang F, Moss LG, Phillips GN Jr. The molecular structure of Green Fluorescent Protein. Nat Biotech 1996;14:1246–1251.
4. Brejc K, Sixma TK, Kitts PA, Kain SR, Tsien RY, Ormö M, Remington SJ. Structural basis for dual excitation and photoisomerization of the Aequorea Victoria Green Fluorescent Protein. Proc Natl Acad Sci USA 1997;94:2306–2311.
5. Palm GJ, Zdanov A, Gaitanaris GA, Stauber R, Pavlakis GN, Wlodawer A. The structural basis for spectral variations in Green Fluorescent Protein. Nat Struct Biol 1997;4:361–365.
6. Elsliger MA, Wachter RM, Hanson GT, Kallio K, Remington SJ. Structural and spectral response of Green Fluorescent Protein variants to changes in pH. Biochemistry 1999;38:5296–5301.
7. Weber W, Helms V, McCammon JA, Langhoff PW. Shedding light on the dark and weakly fluorescent states of Green Fluorescent Proteins. Proc Natl Acad Sci USA 1999;96:6177–6182.
8. Voityuk AA, Michel-Beyerle ME, Rosch N. Protonation effects on the chromophore of Green Fluorescent Protein. Quantum chemical study of the absorption spectrum. Chem Phys Lett 1997;272:162–167.
9. Tsien RY. The Green Fluorescent Protein. Annu Rev Biochem 1998;67:509–544.
10. Wachter RM, Elsliger MA, Kallio K, Hanson GT, Remington SJ. Structural basis of spectral shifts in the yellow-emission variants of Green Fluorescent Protein. Structure 1998;6:1267–1277.
11. Kummer AD, Wiehler J, Rehaber H, Kompa C, Steipe B, Michel-Beyerle ME. Effects of threonine 203 replacements on excited-state dynamics and fluorescence properties of the Green Fluorescent Protein (GFP). J Phys Chem B 2000;104:4791–4798.
12. Kummer AD, Kompa C, Lossau H, Pollinger-Dammer F, Michel-Beyerle ME, Silva CM, Bylina EJ, Coleman WJ, Yang MM, Youvan DC. Dramatic reduction in fluorescence quantum yield in mutants of Green Fluorescent Protein due to fast internal conversion. Chem Phys 1998;237:183–193.
13. Case D, Pearlman D, Caldwell J, Cheatham T III, Ross W, Simmerling C, Darden T, Merz K, Stanton R, Cheng A, Vincent J, Crowley M, Tsui V, Radmer R, Duan Y, Pitera J, Massova I, Seibel G, Singh U, Weiner P, Kollman PA. Amber 6.0. 1999.
14. Cinelli R. AG, Pellegrini V, Ferrari A, Faraci P, Nifosì R, Tyagi M, Giacca M, Beltram F. Green Fluorescent Proteins as optically controllable elements in bioelectronics. Appl Phys Lett 2001;79:3353–3355.
15. Dickson RM, Cubitt AB, Tsien RY, Moerner WE. On/off blinking and switching behaviour of single molecules of Green Fluorescent Protein. Nature 1997;388:355–358.
16. Helms V, Straatsma TP, McCammon JA. Internal dynamics of Green Fluorescent Protein. J Phys Chem B 1999;103:3263–3269.
17. Reuter N, Lin H, Thiel W. Green Fluorescent Proteins: Empirical force field for the neutral and deprotonated forms of the chromophore. Molecular dynamics simulations of the Wild Type and S65T mutant. J Phys Chem B 2002;106:6310–6321.
18. Haupts U, Maiti S, Schwille P, Webb WW. Dynamics of fluorescence fluctuations in Green Fluorescent Protein observed by fluorescence correlation spectroscopy. Proc Natl Acad Sci USA 1998;95:13573–13578.
19. Schwille P, Kummer S, Heikal AA, Moerner WE, Webb WW. Fluorescence correlation spectroscopy reveals fast optical excitation-driven intramolecular dynamics of Yellow Fluorescent Proteins. Proc Natl Acad Sci USA 2000;97:151–156.

20. Garcia-Parajo MF, Segers-Nolten GM, Veerman JA, Greve J, van Hulst NF. Real-time light driven dynamics of the fluorescence emission in single Green Fluorescent Protein molecules. Proc Natl Acad Sci USA 2000;97:7237–7242.
21. Peterman E. JG, Brasselet S, Moerner WE. The fluorescence dynamics of single molecules of Green Fluorescent Protein. J Phys Chem A 1999;103:10553–10560.
22. InsightII, Accelrys Inc. 2001.
23. Berman H, Westbrook J, Feng Z, Gilliland G, Bhat T, Weissig H, Shindyalov I, Bourne P. The Protein Data Bank. Nucleic Acids Res 2000;28:235–242.
24. van Thor JJ, Pierik AJ, Nugteren-Roodzant I, Xie A, Hellingwerf KJ. Characterization of the photoconversion of Green Fluorescent Protein with FTIR spectroscopy. Biochemistry 1998;37:16915–16921.
25. Yoo H, Boatz JA, Helms V, McCammon JA, Langhoff PW. Chromophore protonation states and the proton shuttle mechanism in Green Fluorescent Protein: inferences drawn from ab initio theoretical studies of chemical structures and vibrational spectra. J Phys Chem B 2001;105:2850–2857.
26. MacKerell AD Jr, Bashford D, Bellott RL, Dunbrack RL Jr, Evanseck JD, Field MJ, Fischer S, Gao J, Guo H, Ha S, Joseph-McCarthy D, Kuchnir L, Kuczera K, Lau F. TK, Mattos C, Michnick S, Ngo T, Nguyen DT, Prodhom B, Reiher WE III, Roux B, Schlenkrich M, Smith JC, Stote R, Straub J, Watanabe M, Wiorkiewicz-Kuczera J, Yin D, Karplus M. All-atom empirical potential for molecular modeling and dynamics studies of proteins. J Phys Chem B 1998;102:3586–3616.
27. Bayly C, Cieplak P, Cornell W, Kollman P. A well-behaved electrostatic potential based method using charge restraints for determining atom-centered charges. J Phys Chem 1993;97:10269–10280.
28. Kollman PA. Free energy calculations: applications to chemical and biochemical phenomena. Chem Rev 1993;93:2395–2417.
29. Humphrey W, Dalke A, Schulten K. Vmd—visual molecular dynamics. J Mol Graph 1996;14:33–38.
30. Scharnagl C, Raupp-Kossmann R, Fischer SF. Molecular basis for pH sensitivity and proton transfer in Green Fluorescent Protein: protonation and conformational substates from electrostatic calculations. Biophys J 1999;77:1839–1857.
31. Cotlet M, Hofkens J, Maus M, Gensch T, Van der Auweraer M, Michiels J, Dirix G, Van Guyse M, Vanderleyden J, Visser AJWG, De Schryver FC. Excited-state dynamics in the Enhanced Green Fluorescent Protein mutant probed by picosecond time-resolved single photon counting spectroscopy. J Phys Chem B 2001;105:4999–5006.
32. Nifosì R, Ferrari A, Arcangeli C, Tozzini V, Pellegrini V, Beltram F. Photoreversible dark state in a tristable green fluorescent protein variant. J Phys Chem B 2003;107:1679–1684.
33. Cubitt AB, Woollenweber LA, Heim R. Understanding structure-function relationships in the Aequorea Victoria Green Fluorescent Protein. Methods Cell Biol 1999;58:19–30.
34. Heikal AA, Hess ST, Baird GS, Tsien RY, Webb WW. Molecular spectroscopy and dynamics of intrinsically fluorescent proteins: coral red (dsred) and yellow (citrine). Proc Natl Acad Sci USA 2000;97:11996–12001.